JOURNAL OF MAGNETIC RESONANCE **133,** 341–351 (1998)
ARTICLE NO. MN981488

Application of Rotor-Synchronized Amplitude-Modulated Cross-Polarization in a ^{13}C–^{1}H Spin Pair under Fast Magic-Angle Spinning

Jésus Raya and Jérôme Hirschinger[1]

Institut de Chimie, UMR 7510 CNRS, Bruker S.A., Université Louis Pasteur, BP 296, 67008 Strasbourg Cedex, France

Received November 26, 1997

Rotor-synchronized amplitude-modulated Hartmann–Hahn cross-polarization has been applied under fast magic-angle spinning to a powder sample of ferrocene. The influence on the cross-polarization process of the heteronuclear double quantum (flop–flop) transitions induced by the amplitude modulation for low ratios of the radiofrequency-field strength to the spinning speed is studied in details. The experimental data are in good agreement with theoretical calculations for a two-spin $\frac{1}{2}$ system, although the intensity of the double quantum transitions is observed to be significantly smaller than expected. Moreover, it is shown that an efficient polarization transfer at the Hartmann–Hahn centerband matching condition as well as a broadening of the matching conditions is obtained by an appropriate partial scaling of the effective radiofrequency fields which minimizes the destructive effect of double quantum cross-polarization.

Key Words: **solid-state NMR; cross-polarization; magic-angle spinning; amplitude-modulation; double quantum cross-polarization.**

INTRODUCTION

Hartmann–Hahn cross-polarization (CP) has become a widespread technique for enhancing the nuclear magnetization of rare spins S with low gyromagnetic ratios using the larger equilibrium polarization of the abundant I spin system (*1–7*). For static samples and continuous-wave cross-polarization (CWCP), it is well known that efficient CP through heteronuclear zero quantum (ZQ or flip–flop) transitions is obtained at the Hartmann–Hahn matching condition $\omega_{1I} = \omega_{1S}$, where ω_{1I} and ω_{1S} are the amplitudes of the radiofrequency (RF) fields applied to the I and S spins (*1, 4*). CP dynamics are very dependent on the relative sizes of the homonuclear (I–I) and heteronuclear (I–S) dipolar interactions. When the fluctuations of the local field governing the spin diffusion process among the I spins are faster than the exchange of magnetization between the two spin systems, the spin-temperature hypothesis can be applied and CP proceeds exponentially as cross-relaxation (*3, 4, 8, 9*). On the other hand, the presence of strong heteronuclear interactions, as in the case of protonated carbons, leads to coherent energy transfer, i.e., an oscillating behavior of the CP dynamics (*4, 10, 11*). An important observation made first by Schaefer and Stejskal (*12*) is that efficient CP transfer also occurs under magic-angle spinning (MAS) conditions, making CP/MAS one of the most widely used techniques in high resolution solid-state NMR (*5, 6*). Indeed, as long as the spinning speed ω_r is smaller than the homogeneous I-spin linewidth, CP is not significantly affected by MAS. However, this condition is not fulfilled for many samples, in particular when the dipolar interactions are averaged by molecular motions. Moreover, with the increasing availability of ultrahigh magnetic fields (up to 19 T) (*13*), it is often necessary to use spinning speeds exceeding both the I–I and I–S dipolar interactions in order to fully average chemical shift anisotropies. In this case, Stejskal *et al.* (*14*) have first shown that the single Hartmann–Hahn condition splits into a series of new ''sideband'' matching conditions $\omega_{1S} - \omega_{1I} = n\omega_r$ with $n = 0, \pm1, \pm2, \ldots$. With increasing spinning speed, polarization transfer becomes ineffective at centerband matching ($n = 0$) and efficient CP is obtained only at the first- and second-order sidebands ($n = \pm1, \pm2$) (*15–18*). Furthermore, for low ratios of the RF-field strength to the rotation frequency, Meier (*15*) has demonstrated that double quantum (DQ or flop–flop) CP occurs at the Hartmann–Hahn conditions $\omega_{1I} + \omega_{1S} = n\omega_r$ and gives a polarization transfer of opposite sign to the one driven by the flip-flop Hamiltonian. In practice, as spin diffusion is slowed down by MAS, sideband matching is difficult because of the excessive sensitivity of the matching condition to the RF-field amplitudes of the two channels. Consequently, the CP efficiency is strongly reduced by RF-field inhomogeneities, chemical shifts and fluctuations in both RF power and the spinning speed.

Recently, several techniques have been developed to enhance the rate of cross-polarization and to broaden the width of the Hartmann–Hahn matching conditions under fast MAS. Mechanical solutions involving a flip of the rotational axis away from the magic angle during CP or the use of a combi-

[1] To whom correspondence should be addressed.

1090-7807/98 $25.00

nation of low-speed CP and high-speed data acquisition were proposed by Maciel and co-workers (*19, 20*). Alternatively, a pulse sequence using simultaneous phase inversion of both spin-locking fields (SPICP) was shown to provide compensation for Hartmann–Hahn mismatch in fast-rotating samples (*16, 21, 22*). In fact, SPICP, which is a rotor-synchronized version of the mismatch-optimized *IS* transfer (MOIST) sequence originally developed for static samples (*11*) or in liquids (*23*), can be regarded as a special double amplitude-modulated cross-polarization (D-AMCP) pulse sequence (*24*). Amplitude-modulated cross-polarization (AMCP) has been studied in detail by Hediger *et al.* (*24, 25*), who have demonstrated using the Floquet formalism (*26*) that efficient polarization transfer at the original centerband matching condition can be achieved with AMCP and that the width of the matching conditions is efficiently broadened by rotor-synchronized 180° phase shifts. The technique for synchronous accumulation of polarization under MAS developed by Pratima and Ramanathan (*27*) may be also considered as a special AMCP pulse sequence. Alternatively, the broadening of the sideband matching conditions can be achieved by varying (slowly compared to the MAS rate) the RF field (VACP, RAMP-CP) (*28–30*) or the effective RF field (VEFCP) (*31*). Note that similar results have been obtained by frequency sweep (*32*) and frequency-modulated CP (FMCP) (*33*). Improvement of the CP transfer efficiency by a multiple-pulse approach has also been presented (*34*). Finally, a pulse scheme combining slow and fast RF-field amplitude modulation (AMAP-CP) has been shown to provide efficient centerband CP, broadening of the Hartmann–Hahn matching condition, as well as enhanced quasi-equilibrium polarization (*35*). In the same work, the destructive role of flop–flop transitions in AMCP leading to a decay of the detected *S*-spin signal was also pointed out, and it was observed that the applied RF fields should verify the condition $\omega_{1S} + \omega_{1I} > 8\omega_r$ in order to restrict the polarization transfer to the ZQ subspace. However, with the emergence of commercially available high-sensitivity spinning assemblies easily capable of speeds in the 10–20 kHz range, the required RF-field strengths may have to be prohibitively high. Furthermore, since increasing instabilities of the RF fields are generally observed at higher spin-lock powers (*15, 35*) and because the width of the inhomogeneous RF distribution is proportional to the RF field strength (see Experimental), the RF power should in principle be minimized. Hence, it is of interest to examine the efficiency of AMCP sequences for low ratios of the RF-field amplitude to the spinning speed.

In this paper, we apply rotor-synchronized amplitude-modulated CP sequences (*24, 25*) under fast MAS ($\omega_r = 15$ kHz) to a powder sample of ferrocene. In this system, the heteronuclear ^{13}C–^{1}H coupling between directly bonded atoms exceeds all other couplings (*10, 11, 36*). The resulting two-stage character of the polarization transfer has been previously studied in both static and rotating samples (*11, 37–39*). Note that a similar behavior has been observed for rigid or semirigid CH_n groups in many other organic solids (*40–49*). Both the reintroduction of efficient CP at the centerband matching condition and the broadening of the matching conditions are examined with special attention given to the influence of flop–flop transitions. The experimental results are directly compared with calculations for an *IS* two-spin $\frac{1}{2}$ system.

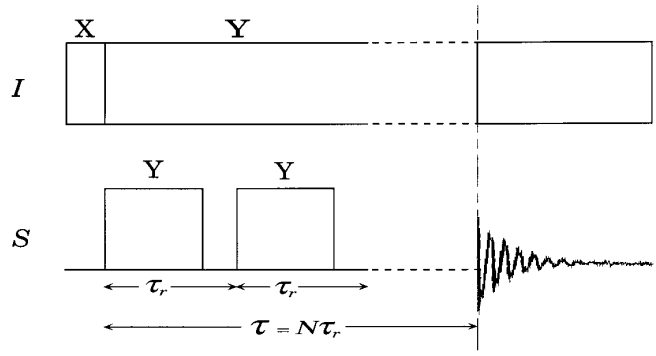

FIG. 1. S-AMCP(p, 0) pulse sequence where p indicates the fraction of the MAS period τ_r during which the *S*-spin RF field is applied.

EXPERIMENTAL

The NMR experiments were performed at room temperature on a Bruker Avance DSX-500 spectrometer operating at a ^{13}C frequency of 125.73 MHz and equipped with a Bruker CP/MAS probe using a 4-mm-o.d. rotor. A polycrystalline sample of ferrocene purchased from Fluka was doped with 2% cobaltocene in order to shorten the ^{1}H T_1 spin–lattice relaxation time to about 1 s and was restricted to a small volume (3.5 mm layer) in the center of the coil to reduce RF-field inhomogeneities (*29*). We used the so-called S-AMCP(p, 0) sequence (Fig. 1) proposed by Hediger *et al.* (*24*) employing a MAS-synchronized square-modulation of the spin-lock field on the *S*-spin (^{13}C) channel. This AMCP sequence is particularly simple since the amplitude modulation requires only a single RF power level. The polarization transfer was also rendered less sensitive to exact matching of the RF-field strengths by phase-inverting parts of the S-AMCP(p, 0) amplitude modulation function (*24, 25*), as described in the next section (D-AMCP). The proton 90° pulse and decoupling during acquisition were both fixed at an RF-field strength of ~50 kHz. The CP matching profile (*25*) at a given mixing time τ was obtained by measuring the integrated peak intensity in the carbon spectrum as a function of the proton RF-field strength ω_{1I} while keeping constant the RF amplitude of the carbon channel ω_{1S} at 50.5 kHz. Usually, the opposite choice (constant proton irradiation strength) is made in order to ensure good spin-lock properties for the entire CP matching profile and mixing time range (*11, 14–18, 28–31, 33*). However, in our case, both $T_{1\rho}(^{1}H)$ measurements and calculated CP matching profiles

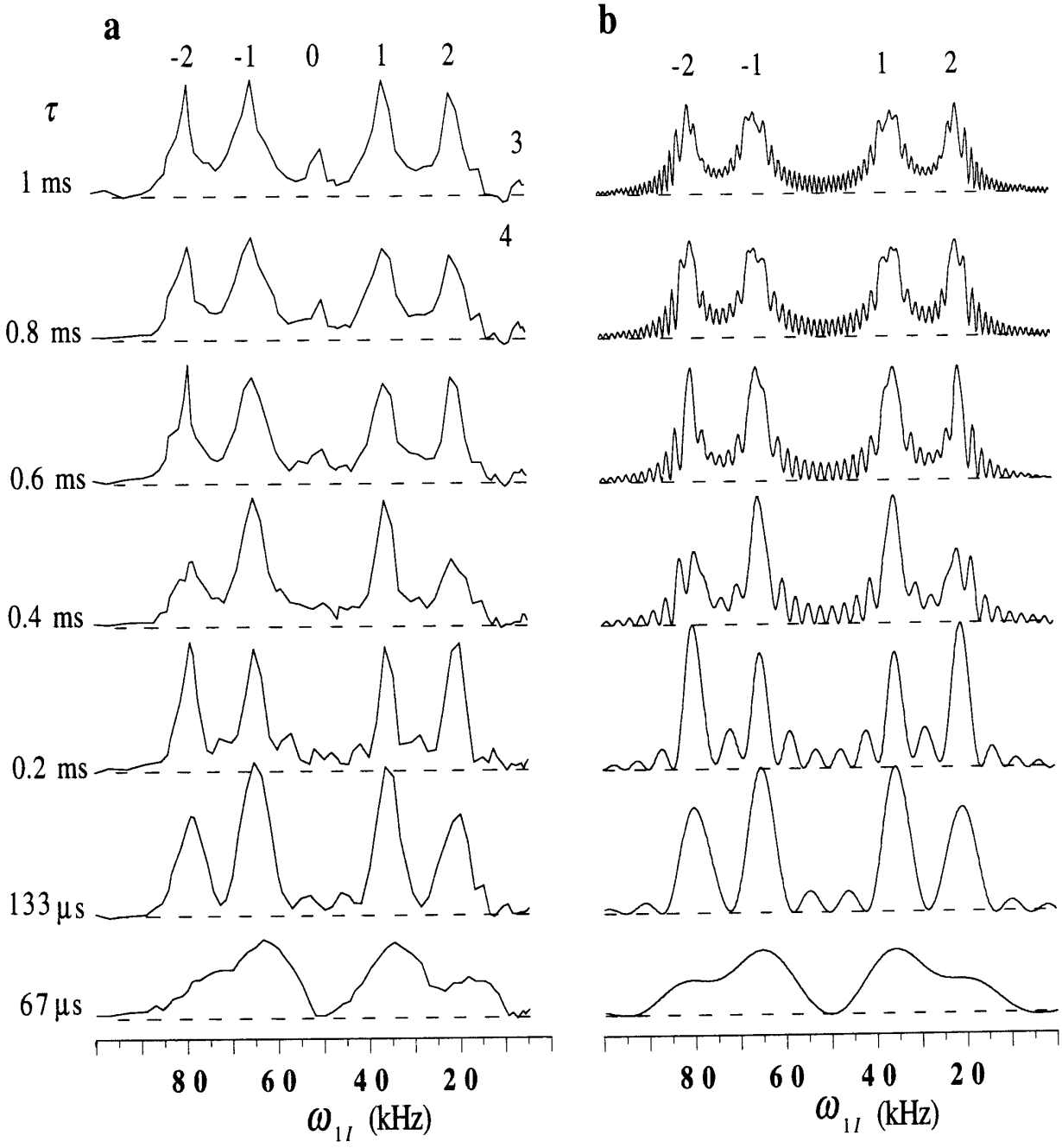

FIG. 2. (a) Integrated line intensity of the carbon resonance in ferrocene as a function of the proton RF-field strength ω_{1I} (CP matching profile) at different contact times τ for the CWCP sequence at a spinning speed of 15 kHz. The carbon RF-field ω_{1S} is equal to 50.5 kHz. (b) Calculated CWCP matching profiles for a ^{13}C–^{1}H pair with an internuclear distance of 1.09 Å. The CP matching profiles are plotted on the same amplitude scale so that they can be directly compared.

(see below) show that spin-lock losses are weak for the used range of contact times ($\tau \leq 1$ ms). Our choice then has the advantage of minimizing the RF power during the measurement of the CP matching profiles. In fact, when using a constant proton RF-field strength, we observed an unexpected asymmetry of the CWCP matching profiles (see below) which we attribute to the large variation of the RF power dissipated into the probe and the receiver preamplifier. The RF fields were calibrated directly with the ferrocene sample using a two-dimensional nutation experiment (*50*) showing that the RF-field inhomogeneity (full width at half-maximum of the nutation peak) is about 5% over the sample volume in both ^{13}C and ^{1}H resonances. We also checked that the RF fields delivered by the linear power amplifier were very stable. Sixty-two exper-

iments with variable ω_{1I} ranging from 4.8 to 100 kHz were recorded for each CP matching profile. The resulting ^{1}H RF-field increments of ca. 1.5 kHz are small enough, considering the accuracy of the RF-field calibration and the RF inhomogeneity. Sixteen scans were added for each experiment with a recycle time of 5 s.

CP matching profiles were computed by integrating numerically the Liouville–von Neumann equation for a rotating ^{13}C–^{1}H two-spin $\frac{1}{2}$ system, as described previously (*44, 49*), neglecting the heteronuclear *J* coupling, the ^{1}H–^{1}H spin diffusion process, and $T_{1\rho}$ relaxation. The time-dependent RF fields of the AMCP sequences, $\omega_{1I}(t)$ and $\omega_{1S}(t)$, were approximated by their expansion in Fourier series. In practice, calculations shows that only the first 10 Fourier coefficients are necessary.

RESULTS AND DISCUSSION

The CWCP matching profiles at different contact times τ in ferrocene are given in Fig. 2. In CW ^{1}H spin-lock experiments, we measured a $T_{1\rho}$ value of 48 ms for $\omega_{1I} = 13$ kHz. Intensity losses due to $T_{1\rho}(^1\text{H})$ relaxation must then be very weak in CWCP experiments for contact times lower than a few milliseconds, at least for $\omega_{1I} > 10$ kHz. The fact that the experimental CWCP matching profiles are symmetric about the static Hartmann–Hahn condition clearly confirms that $T_{1\rho}(^1\text{H})$ effects are negligible for $\tau \leq 1$ ms. Because of the fast rotation of the C_5H_5 rings about the fivefold axis, reducing both the heteronuclear and homonuclear intramolecular interactions by a factor of 2, efficient polarization transfer under fast MAS is obtained at the first- and second-order sidebands (Fig. 2), as previously observed in adamantane (*15–18*). However, because of the presence of well-isolated ^{13}C–^{1}H spin pairs, the situation is quite different in ferrocene. Indeed, Fig. 2 shows that the width of the CP sidebands strongly depends on τ, especially at short contact times. In adamantane, on the other hand, because the homonuclear interactions are dominant, the sideband width is due to the homogeneous *I–I* interactions and is essentially independent of τ (*15*). As demonstrated by the calculations shown in Fig. 2, the variation of the sideband widths and intensities is well described by the oscillatory or coherent polarization transfer in a two-spin system (*7, 10, 11, 16*). Moreover, it is seen that the coherent transfer gives rise to secondary maxima or ''oscillations'' in the CP matching profiles which are clearly apparent in the experimental data at short mixing times, $\tau \leq 0.2$ ms (Fig. 2). These features are no longer visible for $\tau \geq 0.4$ ms since the transient oscillations are known to be invariably damped due to interactions with other spins I_k (spin diffusion) and because of RF inhomogeneity (*10, 11*). In full analogy with the static case, on sideband matching conditions ($n = \pm 1, \pm 2$), a quasi-equilibrium is then reached fairly rapidly where half of the initial polarization of the *I* spin is transferred to the *S* spin (*7, 51*). Note that the quasi-equilibrium polarization can be enhanced by an adiabatic

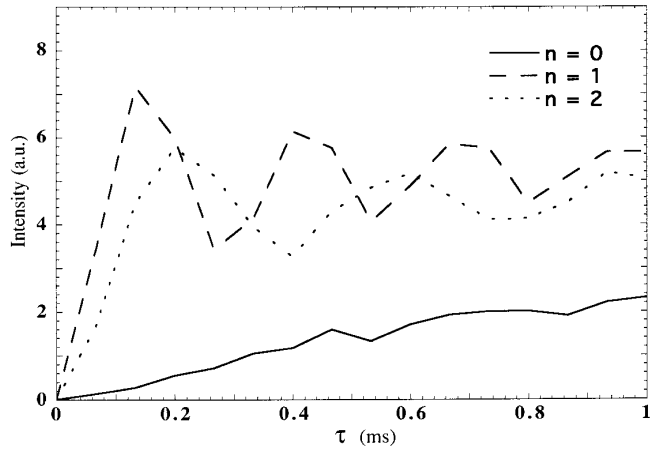

FIG. 3. The CWCP ^{13}C magnetization intensity of ferrocene as a function of the contact time τ under different matching conditions with the parameters of Fig. 2. $\omega_{1I} = 49.8$, 36.3, and 21.5 kHz at the $n = 0$, 1, and 2 matching condition, respectively. The CP curves for the $n = -1$ and -2 sidebands (not shown) are identical to the ones obtained for $n = 1$ and 2.

sweep of the RF-field amplitude through a sideband matching condition (*51, 52*). For ferrocene, after strong initial oscillations, the experimental data show that the magnetization stays close to the quasi-equilibrium value for $\tau > 0.5$ ms (Fig. 3). However, Fig. 2 shows that the transfer efficiency strongly decreases with a slight deviation from an exact matching condition. Indeed, for $\tau > 0.5$ ms, the full width at half-maximum (FWHM) of the four CP sidebands is about 5 kHz. Hartmann–Hahn CWCP matching then requires a rather stable and homogeneous RF field. Note that the matching conditions are expected to be even narrower in the presence of additional fast molecular motion, as is the case for ^{13}C–^{1}H groups in various organic materials. Some polarization transfer is also obtained at the centerband ($n = 0$) for longer contact times, $\tau \geq 0.6$ ms (Fig. 2). This fact has been previously attributed to the modulation of homonuclear *I–I* interactions by sample spinning (*14*) and to the scalar $^1J_{\text{HC}}$ coupling (*53*), leading to a transfer rate constant much smaller than at the $n = \pm 1$ and ± 2 matching conditions (Fig. 3). A close inspection of Fig. 2 shows that the ^{1}H–^{1}H couplings are also responsible for the appearance of weak $n = \pm 3$ and 4 sidebands. Note that the $n = 4$ matching condition, which would be positioned at a value corresponding to a negative proton field strength, is driven by the flop–flop part of the Hamiltonian and, thus, appears with negative intensity at a frequency position ''folded back'' at the right margin of the CP profile (*15*). Of course, CWCP at the centerband and at the $|n| > 2$ sideband matching conditions cannot be accounted for by our computations using the two-spin approximation (Fig. 2). Nevertheless, the good agreement between experimental and calculated CP matching profiles clearly demonstrates that spin diffusion effects are weak in accordance with the fact that the ^{1}H–^{1}H flip–flop processes are efficiently slowed down by MAS in ferrocene (*36*). Note

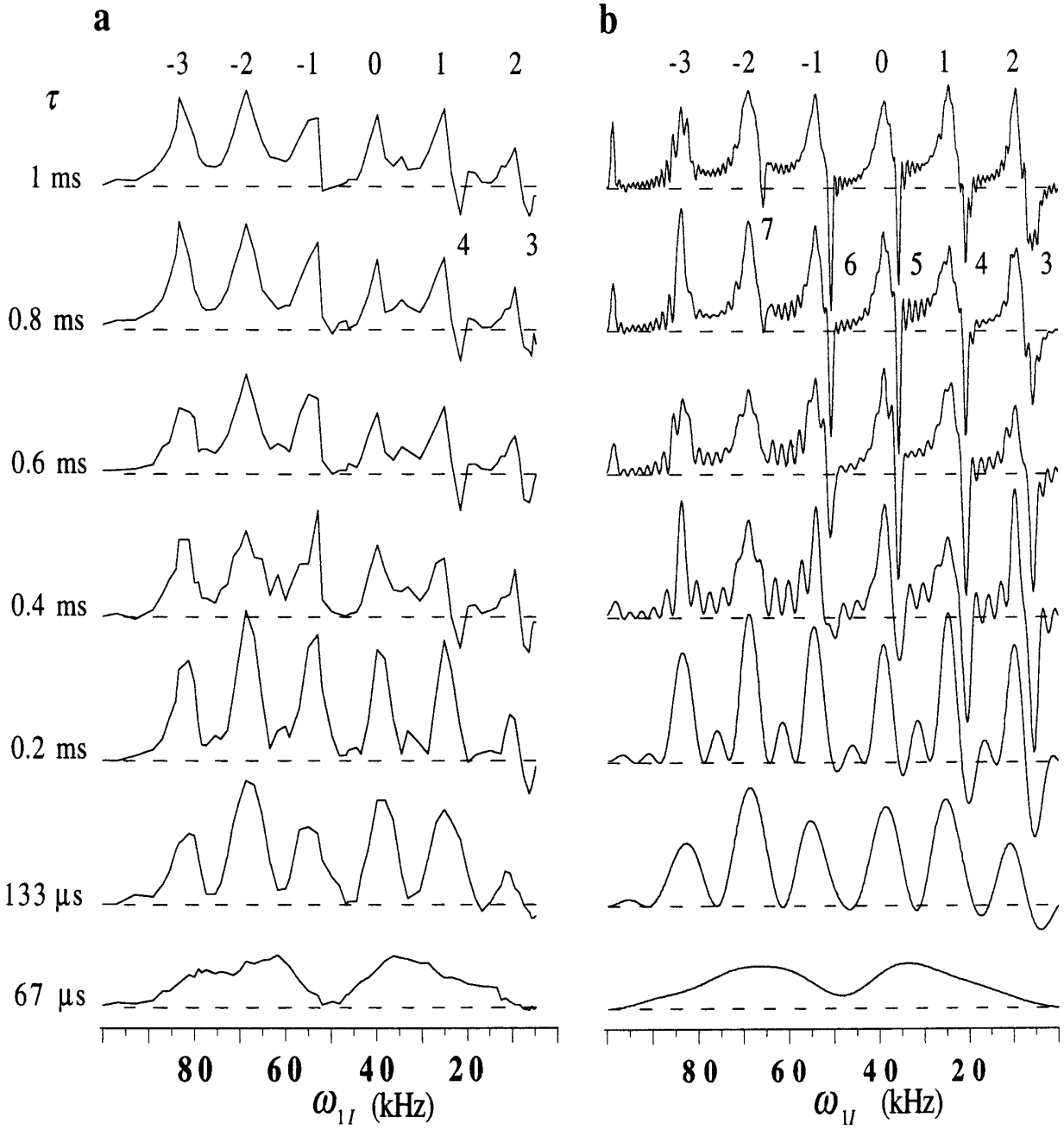

FIG. 4. (a) CP matching profiles at different mixing times τ in ferrocene for the S-AMCP(p, 0) pulse sequence given in Fig. 1 with $p = 0.775$ ($\omega_{1S}^{(0)} = 39.1$ kHz, $\omega_r = 15$ kHz). (b) Calculated CP matching profiles. The CP matching profiles are plotted on the same amplitude scale as in Fig. 2.

finally that double quantum CWCP is not observed in the calculated CP matching profiles since the applied RF field ω_{1S} is larger than twice the spinning frequency (*15*).

As demonstrated by Hediger *et al.* (*24, 25*), efficient CP under fast MAS at the original Hartmann–Hahn condition can be reintroduced using AMCP pulse sequences like the one pictured in Fig. 1, S-AMCP(p, 0). Cross-polarization performed with centerband matching ($n = 0$) is preferable because it is insensitive to the rotation frequency and is also less sensitive to RF inhomogeneities than with sideband matching (*16, 24, 25*). In AMCP, the matching conditions corresponding to a nonvanishing effective flip–flop Hamiltonian are defined by $\omega_{1S}^{(0)} - \omega_{1I}^{(0)} = n\omega_r$, where $\omega_{1I}^{(0)}$ and $\omega_{1S}^{(0)}$ are the mean values of the time-dependent RF fields $\omega_{1I}(t)$ and $\omega_{1S}(t)$ over one rotor period (zero-order Fourier coefficients) (*24, 25*). In particular, CP at the centerband matching condition, $\omega_{1I}^{(0)} =$

$\omega_{1S}^{(0)}$, becomes allowed. Figure 4 shows the CP matching profiles resulting from the application of the S-AMCP(p, 0) pulse sequence (Fig. 1) with $p = 0.775$ to ferrocene at a spinning frequency of 15 kHz. Indeed, considerable polarization transfer at the $n = 0$ matching condition, $\omega_{1I} = p\omega_{1S} = 39.1$ kHz, is obtained already after two rotor cycles (133 μs) and the CP efficiency at the centerband is now comparable to the one obtained with sideband matching in CWCP (Fig. 2). Although p was not optimized, we observed that both the initial CP rate and width of the centerband matching condition were significantly smaller for $p = 0.925$ (data not shown). An identical quasi-equilibrium value was nevertheless obtained, as expected in an isolated two-spin system. Optimization of the amplitude modulation then appears to be less critical in ferrocene than in samples such as adamantane where the *S*-spin magnetization is proportional to the initial transfer rate constant (*25*). However, because the RF modulation inevitably introduces higher-order CP sidebands ($|n| > 2$), a ''foldback'' behavior may arise at the matching conditions $\omega_{1S}^{(0)} + \omega_{1I}^{(0)} = n\omega_r$ from double-quantum processes (*35*). Since the quasi-equilibrium state polarization reached after CP due to flop–flop transitions is of opposite sign to the one resulting from flip–flop CP (*15*), the ZQ and DQ terms may compete and lead to an undesired loss of magnetization (*35*). In fact, under simultaneous ZQ and DQ matched conditions, the populations at the quasi-equilibrium state in both the ZQ and DQ subspaces are predicted to be equalized so that no polarization is finally transferred to the *S* spin (*22, 51*). Clearly, the CP transfer must be restricted to the *ZQ* subspace not only to obtain an optimal CP transfer, but also to maintain a large *S*-spin magnetization for resonances with fast CP building rates (e.g., protonated carbons) at the long contact times required to polarize signals with slower CP rates (e.g., nonprotonated carbons) (*35*). The experimental data of Fig. 4 clearly demonstrate the presence of double quantum CP at the matching conditions $n = 3$ and 4. Nevertheless, the intensities of the folded-back sidebands are seen to be lower than expected from the calculations. This is particularly true for the $n = 5$ and 6 sidebands at long mixing times ($\tau > 0.5$ ms) which are not detected experimentally (Fig. 4). The reason for this fact is not clearly understood, although it may be caused by RF-field inhomogeneities, pulse imperfections, and the ^{1}H–^{1}H dipolar interactions which are not taken into account in the calculations. Moreover, the quasi-equilibrium polarization obtained at both the centerband and $n > 0$ sideband matching conditions is significantly less than expected from the computations (Fig. 4) as well as than the one obtained experimentally in CWCP for $n = \pm 1$ and ± 2 (compare Figs. 3 and 5). Since ^{1}H spin-locking during the S-AMCP(p, 0) sequence is as good as in CWCP, this loss of magnetization must be attributed to flop–flop transitions, as already noticed by Hediger *et al.* (*35*). Indeed, in Fig. 4, the ZQ and DQ matching conditions are only $\sim$3 kHz apart from each other so that there is some overlap, especially when considering RF-field inhomogeneities. Of course, this

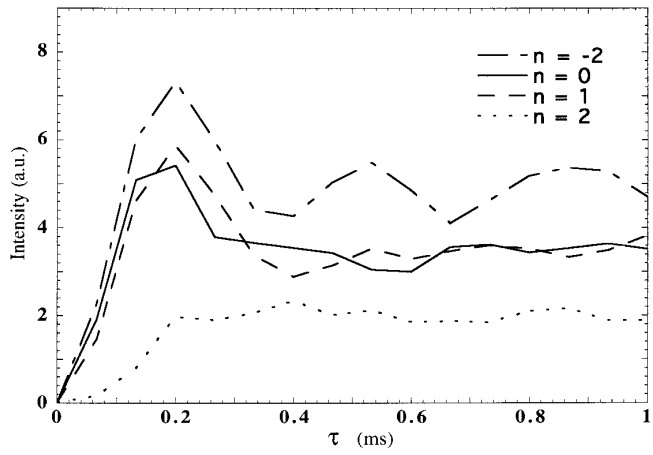

FIG. 5. ^{13}C signal intensity as a function of the mixing time τ in ferrocene under different matching conditions for the S-AMCP(p, 0) pulse sequence with the parameters of Fig. 4. $\omega_{1I} = 68.8$, 39.9, 25.2, and 9.5 kHz at the $n = -2$, 0, 1, and 2 matching conditions, respectively. The same amplitude scale as in Fig. 3 has been used.

overlap can be reduced by changing (preferably increasing) the mean value of the RF field $\omega_{1S}^{(0)}$. From the experimental results of Fig. 4, it may be inferred that the flop–flop transitions should be negligible for $\omega_{1S}^{(0)} + \omega_{1I}^{(0)} > 8\omega_r$ ($\omega_{1I}^{(0)}$, $\omega_{1S}^{(0)} > 60$ kHz), in agreement with previous AMCP experimental results and calculations of the dipolar coupling elements in the Floquet space (*35*). However, since the second goal pursued by AMCP is to broaden the matching conditions, we prefer to address this problem in the following using double amplitude-modulated CP (D-AMCP) pulse sequences.

It has been shown (*25*) that the matching conditions can be widened at will in D-AMCP by reducing $\omega_{1I}^{(0)}$ and $\omega_{1S}^{(0)}$ relative to the mean RF magnitudes $\overline{|\omega_{1I}|}$ and $\overline{|\omega_{1S}|}$, which is most easily achieved by phase-inverting parts of the spin-locking fields. Indeed, the separation between the sidebands of the matching profile and, at the same time, the widths of the matching conditions are then increased by the scaling factor $1/q$, where q is defined by $(\omega_{1S}^{(0)} - \omega_{1I}^{(0)})/(\overline{|\omega_{1S}|} - \overline{|\omega_{1I}|})$. In particular, when $q = 0$, the Hartmann–Hahn condition $\omega_{1I}^{(0)} = \omega_{1S}^{(0)} = 0$ is fulfilled for any applied RF-field strengths and the CP matching profile is expected to be infinitely broad. However, in practice, the applicability of AMCP with a low value of q is limited by the strength of the *I*-spin homonuclear dipolar coupling since the effective spin-lock field is then weak (*24, 25*). Moreover, since the entire CP profile is scaled by the factor $1/q$ along the frequency axis, the destructive foldback effect of flop–flop processes is expected to be important in D-AMCP for low ratios of the RF field amplitude to the spinning rate. This fact is clearly evidenced by a decay of the sum polarization in our computations for an *IS* two-spin system. Indeed, in principle, the RF fields must then be very strong ($\overline{|\omega_{1S}|} + \overline{|\omega_{1I}|} > 8\omega_r/q$) to avoid the DQ matching conditions. For ferrocene at $\omega_r = 15$ kHz, we have effectively

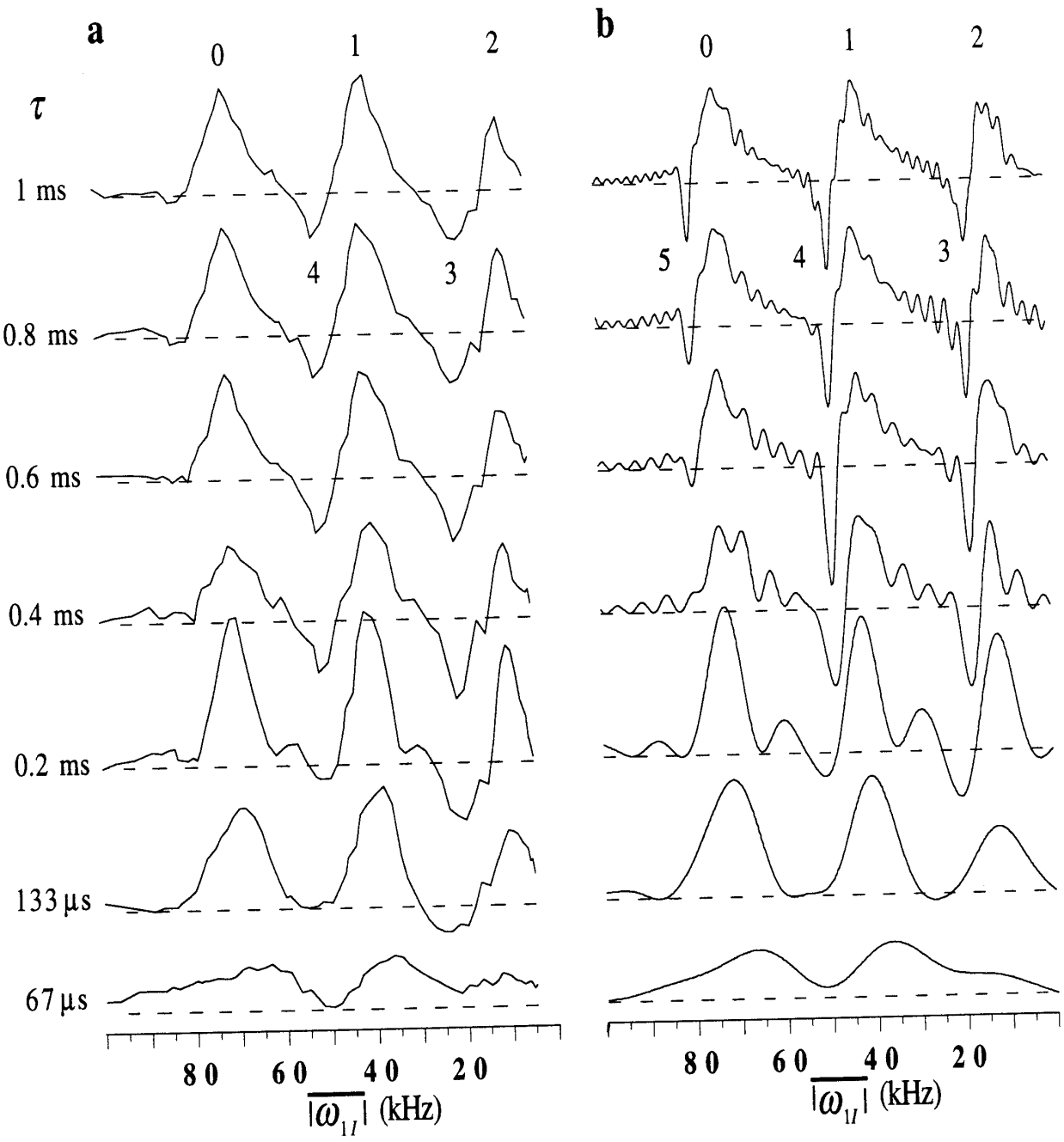

FIG. 6. (a) CP matching profiles at different mixing times τ in ferrocene obtained with the D-AMCP(p, 0, q_I, q_S) pulse sequence with $p = 0.775$, $q_I = 0.490$, and $q_S = 0.923$. (b) Calculated CP matching profiles. The CP matching profiles are plotted on the same amplitude scale as in Fig. 2.

observed that D-AMCP sequences with $q = 0$ lead, after a rapid initial increase during the first three rotor cycles, to a decay of the *S*-spin polarization toward a quasi-equilibrium magnetization ($\tau > 0.5$ ms) which is only ~15% of the one obtained experimentally in CWCP (data not shown). As noted by Hediger *et al.* (*25*), it is then necessary to find an acceptable compromise by using an intermediate value of q. If $q = 0.5$, using the same mean carbon RF-field strength as for $q = 1$ in the S-AMCP(p, 0) sequence ($\overline{|\omega_{1S}|} = 39.1$ kHz, Fig. 4), both the $n = 2$, 3, and 4 sidebands are predicted to be folded back in the CP matching profile at $\overline{|\omega_{1I}|} = 20.9$, 50.9, and 80.9 kHz, respectively. $\overline{|\omega_{1S}|}$ should then preferably be increased in order to shift the centerband matching condition toward a higher frequency in the measured CP profile. Alternatively, it is re-

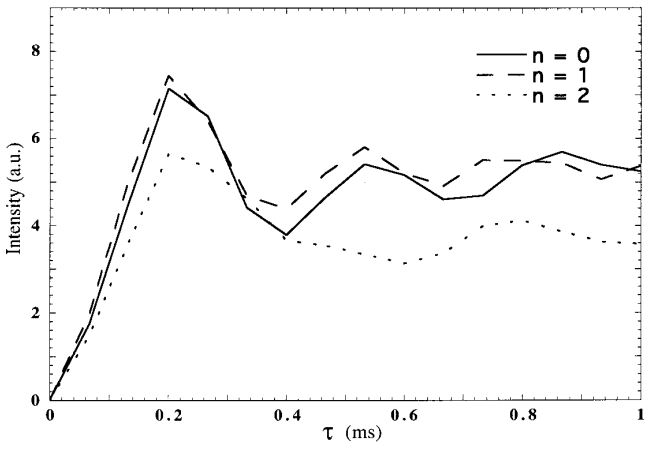

FIG. 7. ^{13}C signal intensity as a function of the mixing time τ in ferrocene under different matching conditions for the D-AMCP(p, 0, q_I, q_S) pulse sequence with the parameters of Fig. 6. $\overline{|\omega_{1I}|}$ = 71.5, 41.9, and 10.5 kHz at the n = 0, 1, and 2 matching conditions, respectively. The same amplitude scale as in Fig. 3 has been used.

marked that such a frequency shift can also be achieved by using different scaling factors on the *I*- and *S*-spin channels, q_I and q_S, since the centerband matching condition is then defined by the relation $q_I\overline{|\omega_{1I}|} = q_S\overline{|\omega_{1S}|}$. Of course, in this case, one can no longer speak of a unique CP profile since the influence on the matching of the mean RF amplitudes, $\overline{|\omega_{1I}|}$ and $\overline{|\omega_{1S}|}$, is different. However, this is a convenient method to produce an ''apparent'' increase of the Hartmann–Hahn frequencies in the matching profile of $\overline{|\omega_{1I}|}$ that is measured here experimentally. Figure 6 shows the CP matching profiles obtained with the D-AMCP(p, 0, q_I, q_S) pulse sequence, i.e., the S-AMCP(p, 0) sequence where the phases of the *I* and *S* RF fields are inverted simultaneously at a fraction of time of each rotor period, τ_p/τ_r = 0.745. Indeed, since we then have q_I = 0.490 and q_S = 0.923, the centerband matching is obtained for $\overline{|\omega_{1I}|}$ = 1.883 $\overline{|\omega_{1S}|}$ = 73.7 kHz, i.e., well above the n = 3 and 4 DQ matching conditions expected at $\overline{|\omega_{1I}|}$ = 18.1 and 48.8 kHz. A good agreement between the experimental and calculated D-AMCP(p, 0, q_I, q_S) profiles is obtained (Fig. 6), though the experimental intensities of the DQ sidebands are smaller than the calculated ones, as already observed with the S-AMCP(p, 0) sequence (Fig. 4). On the other hand, the separation between sidebands (~30 kHz) is effectively multiplied by a scaling factor close to $1/q_I$ = 2.04 and both the centerband and sideband matching conditions are significantly broadened (FWHM of ~10 kHz for $\tau > 0.5$ ms). Moreover, Fig. 7 demonstrates that the transfer efficiency and quasi-equilibrium polarization reached at the centerband and at the n = 1 sideband matching conditions are identical to those observed with CWCP for $n = \pm 1, \pm 2$ (Fig. 3), in agreement with the computations (Figs. 2 and 6). By comparison with the S-AMCP(p, 0) results (Figs. 4, 5), it is seen that the D-AMCP(p, 0, q_I, q_S) pulse sequence which broadens the matching conditions also improves the quasi-equilibrium polarization transfer at the n = 0, 1, and 2 matching conditions. This effect is particularly obvious at low values of the spin-locking field on the *I* spins since the quasi-equilibrium magnetization at the n = 2 sideband ($\overline{|\omega_{1I}|}$ = 10.5 kHz) yielded by the D-AMCP(p, 0, q_I, q_S) sequence (Fig. 7) is approximately twice the one obtained with the S-AMCP(p, 0) sequence (Fig. 5), though $T_{1\rho}(^1\mathrm{H})$ is severely shortened by the phase inversions ($T_{1\rho}(^1\mathrm{H}) \approx 4$ ms for $\overline{|\omega_{1I}|}$ = 13 kHz). Thus, although the undesired foldback behavior of CP sidebands is in principle enhanced when decreasing $\omega_{1I}^{(0)}$ and $\omega_{1S}^{(0)}$ in D-AMCP, it is concluded that the overlap of the ZQ and DQ matching conditions can be efficiently minimized by a proper choice of the scaling parameters q_I and q_S. For example, with (q_I, q_S) = (0.490, 0.923), the n = 1 ZQ matching condition lies more than 10 kHz apart from the n = 3 and 4 DQ sidebands (Fig. 6) and no decay of magnetization due to flop–flop transitions is detected (Fig. 7) although the applied RF-fields are not much higher than the spinning speed ($\overline{|\omega_{1S}|} + \overline{|\omega_{1I}|} < 6\omega_r$). It should be finally mentioned that the quasi-equilibrium polarization obtained at the n = 0 matching condition (Fig. 7) could in principle be enhanced by a factor of 2 combining the rotor-synchronized amplitude modulation with an adiabatic passage of the RF field through the centerband matching condition, as in the AMAP-CP scheme (*35*).

The matching conditions can be further broadened by lowering q_I and q_S. This is illustrated in Fig. 8, which shows the CP matching profiles obtained using the D-AMCP(p, 0, q_I, q_S) sequence with τ_p/τ_r = 0.580 (q_I = 0.160, q_S = 0.497). With these parameters and $\overline{|\omega_{1S}|}$ = 39.1 kHz, only the n = 1 (ZQ) and n = 2 (DQ) sidebands should be observed at $\overline{|\omega_{1I}|}$ = 27.7 and 66.0 kHz in the measured CP profiles (the centerband matching condition is at $\overline{|\omega_{1I}|}$ = 121.5 kHz). Again, both the intensity and the width of the n = 1 sideband are well described by the calculations (Fig. 8), and Fig. 9 shows that the magnetization rapidly reaches the expected quasi-equilibrium state with no significant intensity decay due to either flop–flop transitions or $T_{1\rho}(^1\mathrm{H})$ relaxation. Furthermore, it is seen that the transferred magnetization is only reduced by ~15% when deviating by ±5 kHz from the n = 1 matching condition. Indeed, since the CP profile is approximately scaled by the factor $1/q_I$ = 6.25, the FWHM of the ZQ sideband stays close to 25 kHz over the whole range of measured mixing times (Fig. 8). On the other hand, the n = 2 folded-back sideband which is expected to have a large negative intensity at long contact times ($\tau > 0.5$ ms) is hardly seen experimentally (Fig. 8). Therefore, it is concluded that the large separation between matching conditions obtained at low values of q is useful to reduce the effect of flop–flop transitions in the CP matching profile and that the polarization transfer can be improved by D-AMCP, although the applied RF-field strengths are com-

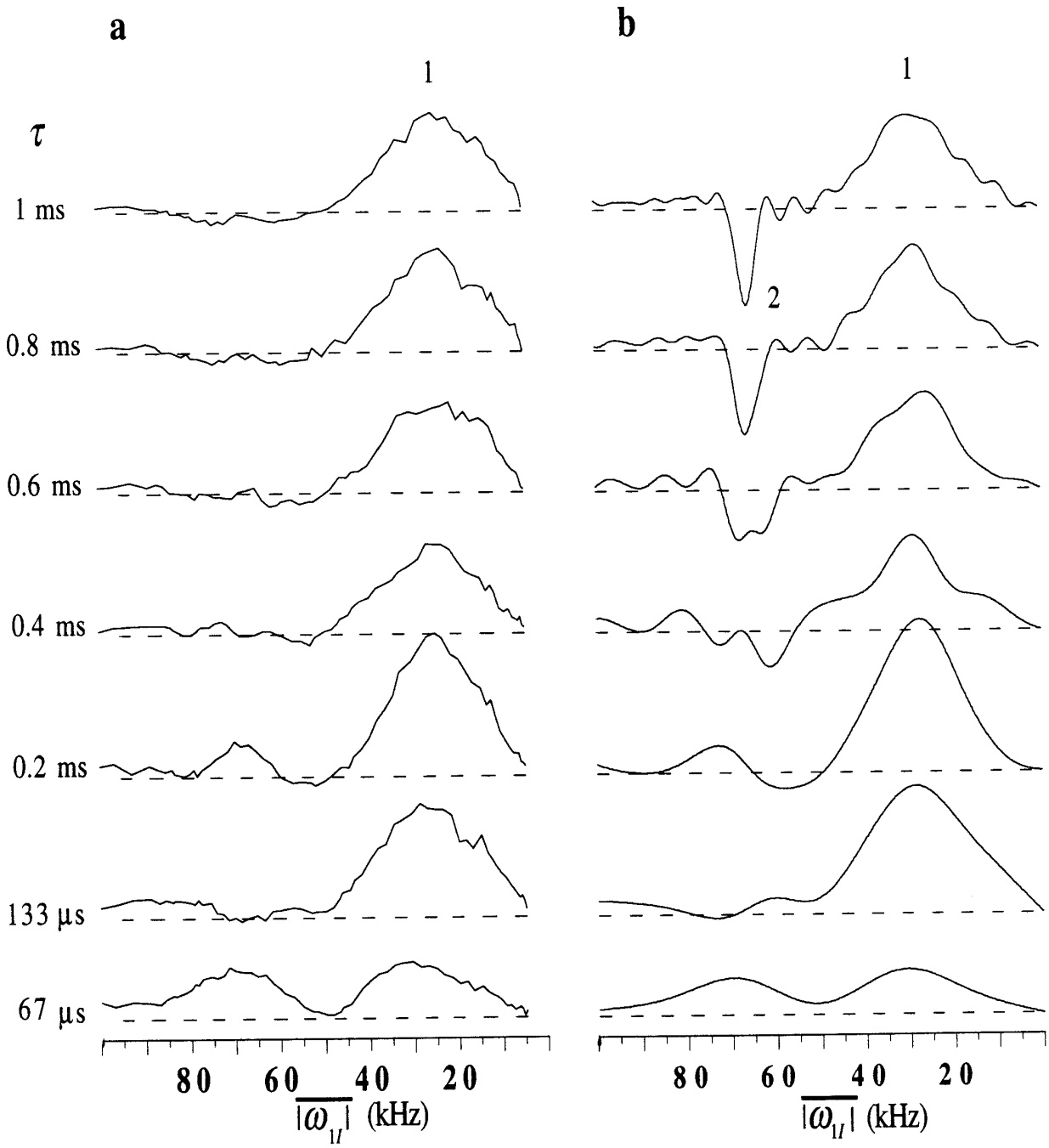

FIG. 8. (a) CP matching profiles at different mixing times τ in ferrocene obtained with the D-AMCP(p, 0, q_I, q_S) pulse sequence with $p = 0.775$, $q_I = 0.160$, and $q_S = 0.497$. (b) Calculated CP matching profiles. The CP matching profiles are plotted on the same amplitude scale as in Fig. 2.

parable to the spinning speed. Indeed, at the $n = 1$ matching condition, we have $|\overline{\omega_{1S}}| + |\overline{\omega_{1I}}| \approx 4\omega_r$ (Fig. 8). Calculations show that a similar transfer efficiency and broadening of the matching conditions (FWHM of ~25 kHz) can be achieved at the preferred centerband with $|\overline{\omega_{1S}}| = |\overline{\omega_{1I}}| \approx 30$ kHz using nonsimultaneous 180° phase shifts on the two channels ($q_S = q_I = q \approx 0.16$). Nevertheless, q should not be lowered below ~0.1 in order to avoid the foldback behavior of the broad matching condition as well as fast $T_{1\rho}(^1\mathrm{H})$ relaxation.

CONCLUSION

Rotor-synchronized double amplitude-modulated cross-polarization has been applied successfully in ferrocene for ratios

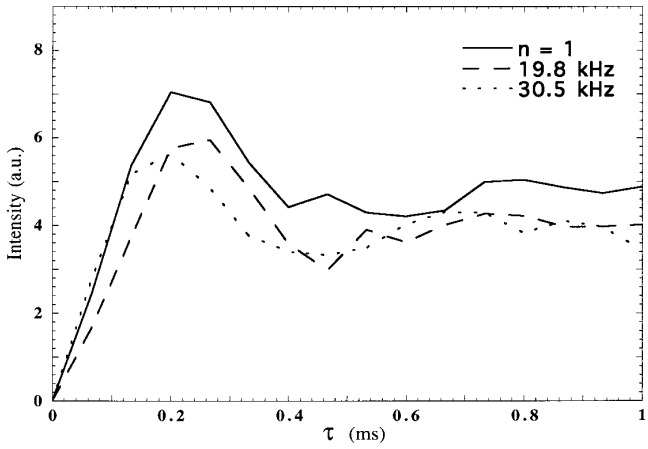

FIG. 9. ^{13}C signal intensity as a function of the mixing time τ in ferrocene for the D-AMCP(p, 0, q_I, q_S) pulse sequence with the parameters of Fig. 8. $|\overline{\omega_{1I}}| = 25.2$ kHz at the $n = 1$ matching condition. The same amplitude scale as in Fig. 3 has been used.

of the radiofrequency-field strength to the spinning speed as low as ~2. Indeed, it has been demonstrated that the destructive effect of the flop–flop transitions which is found to be weaker than predicted by calculations in the two-spin approximation can be efficiently avoided by choosing scaling factors of the effective RF-field levels that minimize the overlap of the zero quantum and double quantum matching conditions. Since broad matching conditions and quasi-equilibrium polarizations are then obtained exclusively through heteronuclear flip–flop processes, high intensity gains may be achieved for resonances having very different cross-polarization building rates (e.g., protonated and nonprotonated carbons).

ACKNOWLEDGMENTS

We thank Professor B. H. Meier for helpful discussions at the solid-state NMR workshop, Les Houches, May 1997. The authors are grateful to the Région Alsace for its participation in the purchase of the Bruker Avance DSX-500 spectrometer.

REFERENCES

1. S. R. Hartmann and E. L. Hahn, *Phys. Rev.* **128,** 2042 (1962).
2. A. Pines, M. G. Gibby, and J. S. Waugh, *J. Chem. Phys.* **56,** 1776 (1972).
3. A. Pines, M. G. Gibby, and J. S. Waugh, *J. Chem. Phys.* **59,** 569 (1973).
4. M. Mehring, ''Principles of High Resolution NMR in Solids,'' Springer, Berlin (1983).
5. C. A. Fyfe, ''Solid State NMR for Chemists,'' CFC Press, Guelph, Ontario, Canada (1983).
6. E. O. Stejskal and J. D. Memory, ''High Resolution NMR in the Solid State: Fundamentals of CP/MAS,'' Oxford Univ. Press, New York (1994).
7. B. H. Meier, Polarization transfer and spin diffusion in solid-state NMR, *in* ''Advances in Magnetic and Optical Resonance'' (W. S. Warren, Ed.), pp. 1–116, Academic Press, New York (1994).
8. D. E. Demco, J. Tegenfeldt, and J. S. Waugh, *Phys. Rev. B* **11,** 4133 (1975).
9. T. T. P. Cheung and R. Yaris, *J. Chem. Phys.* **72,** 3604 (1980).
10. L. Müller, A. Kumar, T. Baumann, and R. R. Ernst, *Phys. Rev. Lett.* **32,** 1402 (1974).
11. M. H. Levitt, D. Suter, R. R. Ernst, *J. Chem. Phys.* **84,** 4243 (1986).
12. J. Schaefer and E. O. Stejskal, *J. Am. Chem. Soc.* **98,** 1031 (1976).
13. S. Steuernagel, H. Förster, F. Engelke, H. D. Zeigler, E. Naumann, and G. Scheler, *Bruker Report* **144,** 30 (1997).
14. E. O. Stejskal, J. Schaefer, and J. S. Waugh, *J. Magn. Reson.* **28,** 105 (1977).
15. B. H. Meier, *Chem. Phys. Lett.* **188,** 201 (1992).
16. X. Wu and K. W. Zilm, *J. Magn. Reson., Ser. A* **104,** 154 (1993).
17. S. Ding, C. A. McDowell, and C. Ye, *J. Magn. Reson., Ser. A* **109,** 1 (1994).
18. S. Ding, C. A. McDowell, and C. Ye, *J. Magn. Reson., Ser. A* **109,** 6 (1994).
19. M. Sardashti and G. E. Maciel, *J. Magn. Reson.* **72,** 467 (1987).
20. R. C. Zeigler, R. A. Wind, and G. E. Maciel, *J. Magn. Reson.* **79,** 299 (1988).
21. T. M. Barbara and E. H. Williams, *J. Magn. Reson.* **99,** 439 (1992).
22. B. Q. Sun, P. R. Costa, and R. G. Griffin, *J. Magn. Reson., Ser. A* **112,** 191 (1995).
23. M. H. Levitt, *J. Chem. Phys.* **94,** 30 (1991).
24. S. Hediger, B. H. Meier, and R. R. Ernst, *Chem. Phys. Lett.* **213,** 627 (1993).
25. S. Hediger, B. H. Meier, and R. R. Ernst, *J. Chem. Phys.* **102,** 4000 (1995).
26. T. O. Levante, M. Baldus, B. H. Meier, and R. R. Ernst, *Mol. Phys.* **86,** 1195 (1995).
27. R. Pratima and K. V. Ramanathan, *Chem. Phys. Lett.* **221,** 322 (1994).
28. O. B. Peersen, X. Wu, I. Kustanovitch, and S. O. Smith, *J. Magn. Reson., Ser. A* **104,** 334 (1993).
29. O. B. Peersen, X. Wu, and S. O. Smith, *J. Magn. Reson., Ser. A* **106,** 127 (1994).
30. G. Metz, X. Wu, and S. O. Smith, *J. Magn. Reson., Ser. A* **110,** 219 (1994).
31. A. C. Kolbert and S. L. Gann, *Chem. Phys. Lett.* **224,** 86 (1994).
32. A. C. Kolbert and A. Bielecki, *J. Magn. Reson., Ser. A* **116,** 29 (1995).
33. R. Fu, P. Pelupessy, and G. Bodenhausen, *Chem. Phys. Lett.* **264,** 63 (1997).
34. H. Geen, J. J. Titman, and H. W. Spiess, *Chem. Phys. Lett.* **213,** 145 (1993).
35. S. Hediger, P. Signer, M. Tomaselli, R. R. Ernst, and B. H. Meier, *J. Magn. Reson.* **125,** 291 (1997).
36. S. Zhang, B. H. Meier, and R. R. Ernst, *Solid State Nucl. Magn. Reson.* **1,** 313 (1992).
37. X. Wu, S. Zhang, and X. Wu, *J. Magn. Reson.* **77,** 343 (1988).
38. X. Wu, X. Xie, and X. Wu, *Chem. Phys. Lett.* **162,** 325 (1989).

39. P. Palmas, P. Tekely, and D. Canet, *J. Magn. Reson., Ser. A* **104,** 26 (1993).

40. X. Wu, S. Zhang, and X. Wu, *Phys. Rev. B* **37,** 9827 (1988).

41. P. Tekely, F. Montigny, D. Canet, and J. J. Delpuech, *Chem. Phys. Lett.* **175,** 401 (1990).

42. X. Wu and K. W. Zilm, *J. Magn. Reson., Ser. A* **102,** 205 (1993).

43. R. Sangill, N. Rastrup-Andersen, H. Bildsoe, H. J. Jakobsen, and N. C. Nielsen, *J. Magn. Reson., Ser. A* **107,** 67 (1994).

44. J. Hirschinger and M. Hervé, *Solid State Nucl. Magn. Reson.* **3,** 121 (1994).

45. P. Tekely, V. Gérardy, P. Palmas, D. Canet, and A. Retournard, *Solid State Nucl. Magn. Reson.* **4,** 361 (1995).

46. P. Palmas, P. Tekely, and D. Canet, *Solid State Nucl. Magn. Reson.* **4,** 105 (1995).

47. G. Hawkes, M. D. Mantle, K. D. Sales, S. Aime, R. Gobetto, and C. J. Groombridge, *J. Magn. Reson., Ser. A* **116,** 251 (1995).

48. R. Pratima and K. V. Ramanathan, *J. Magn. Reson., Ser. A* **118,** 7 (1996).

49. P. Reinheimer, J. Hirschinger, P. Gilard, and N. Goetz, *Magn. Reson. Chem.* **35,** 757 (1997).

50. A. Bax, ''Two-Dimensional NMR in Liquids,'' Delft University Press, Delft (1984).

51. S. Zhang, C. L. Czekaj, and W. T. Ford, *J. Magn. Reson., Ser. A* **111,** 87 (1994).

52. S. Hediger, B. H. Meier, and R. R. Ernst, *Chem. Phys. Lett.* **240,** 449 (1995).

53. A. Verhoeven, R. Verel, and B. H. Meier, *Chem. Phys. Lett.* **266,** 465 (1997).